

Zhang, J., Yang, C., Zhao, L., Zhang, C., Yang, H., Lu, T., Feng, J., Hao, R., Chen, X., and Liu, J., 2023, Hot orogenesis in the Paleoproterozoic: insights from granitic gneiss domes within the Jiao-Liao-Ji belt, North China craton: GSA Bulletin, <https://doi.org/10.1130/B36661.1>.

Supplemental Material

Figure S1. Dependence of the magnetic susceptibility with temperature for representative samples of the Liaoji granitic gneisses.

Figure S2. Magnetic fabric and field fabric of the Hadabei dome.

Figure S3. Shape preferred orientation of magnetite grains and area vs. angle diagrams, and the crystallographic preferred orientation of quartz and magnetite in the Liaoji granitic gneisses.

Figure S4. Field appearance, microscopic characteristics, CL image and zircon U-Pb Concordia diagrams of the dating samples from the Hadabei dome.

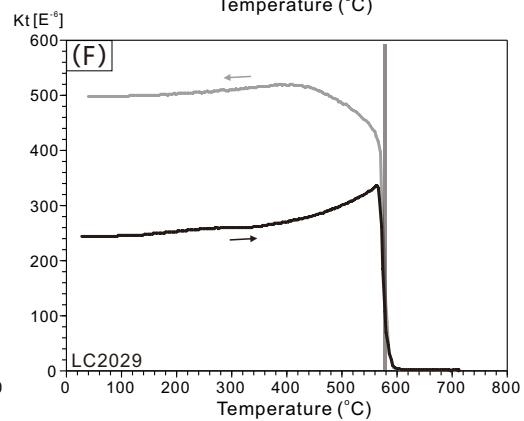
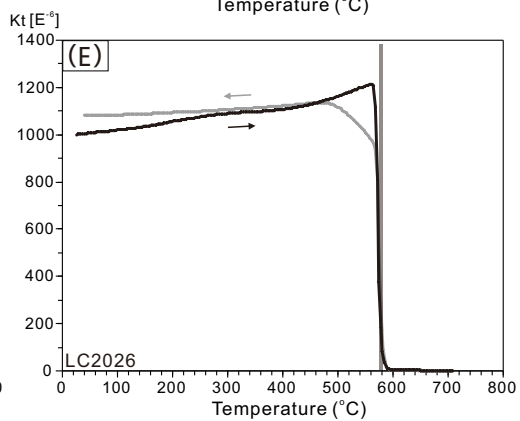
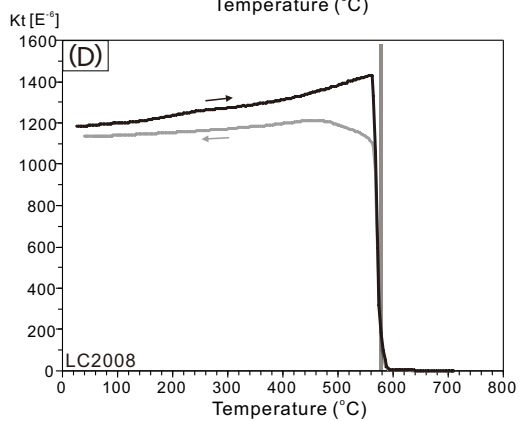
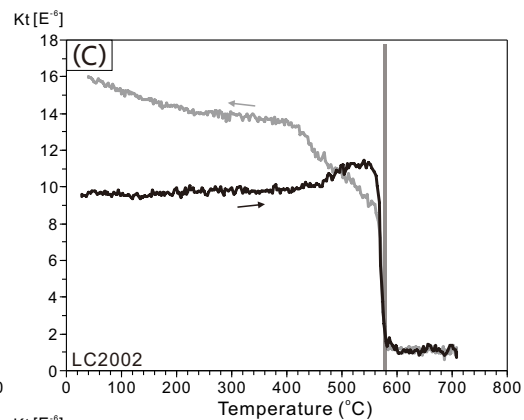
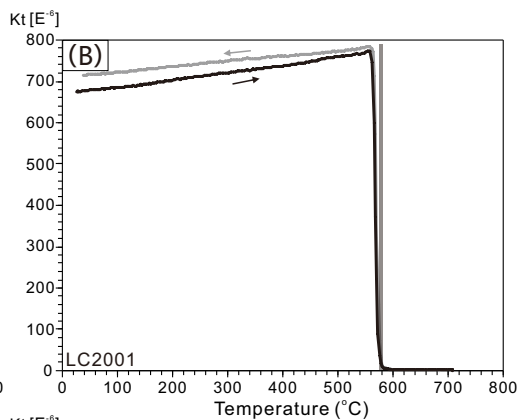
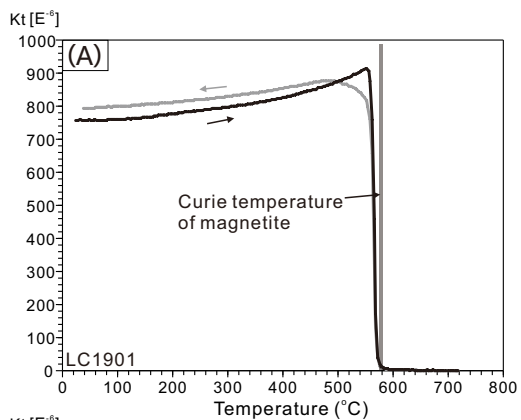
Figure S5. Kinematic map of the northern and southern limbs of the Hadabei dome, with the locations of AMS, field and EBSD sites.

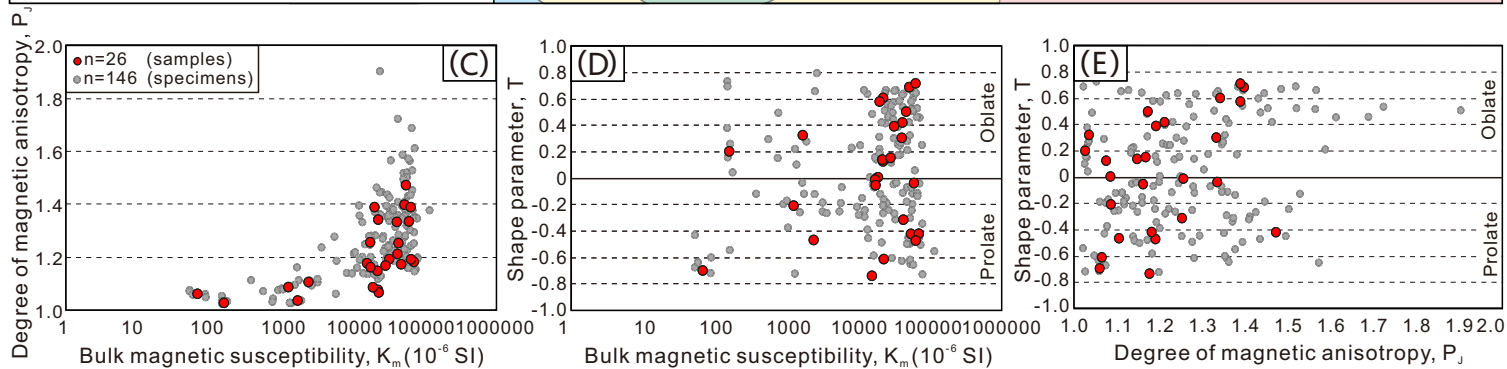
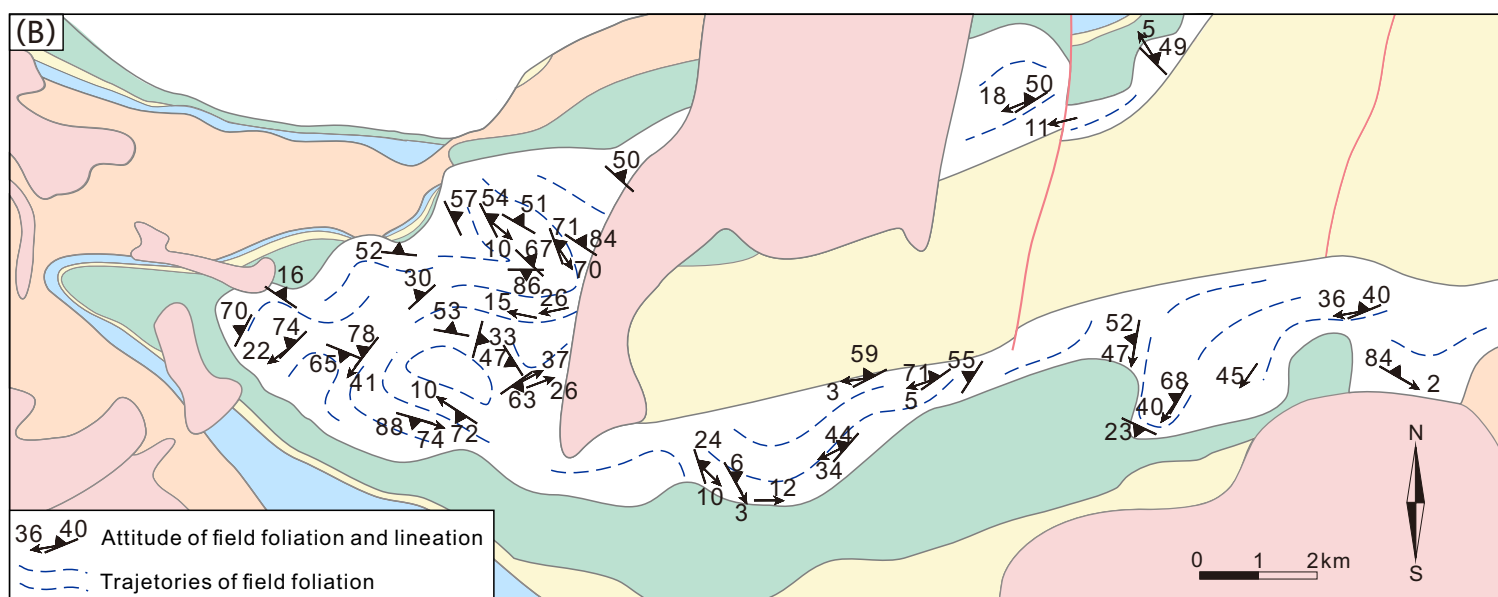
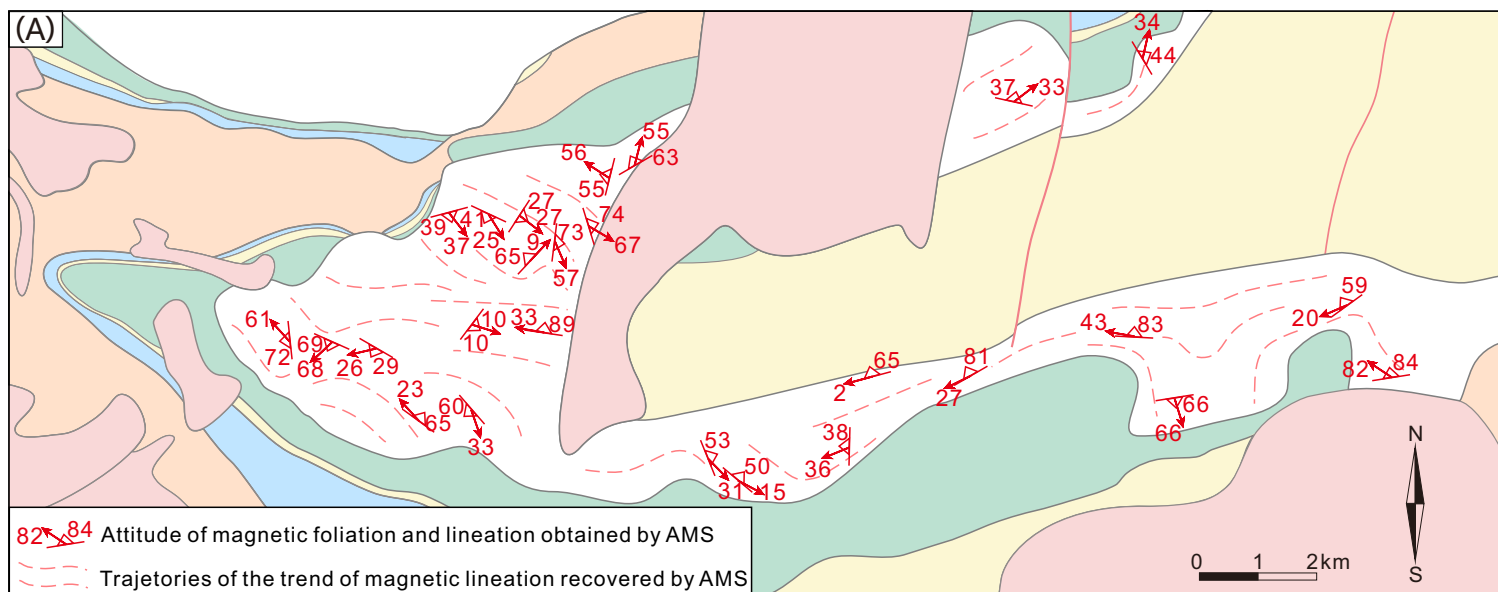
Supplemental Text S1. Sampling strategy and analytical techniques.

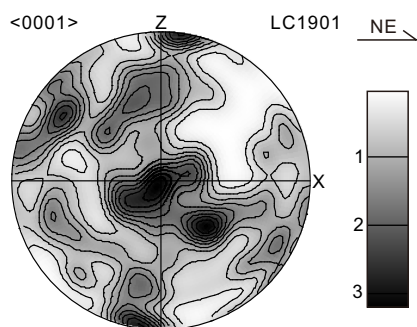
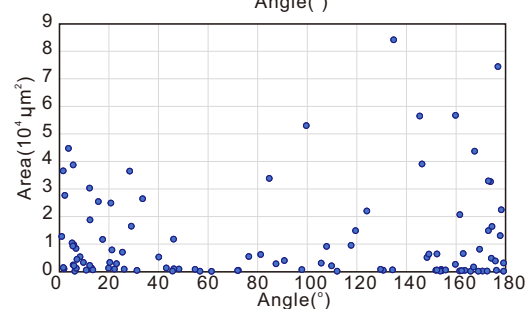
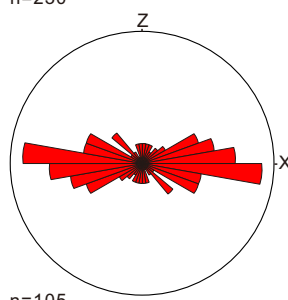
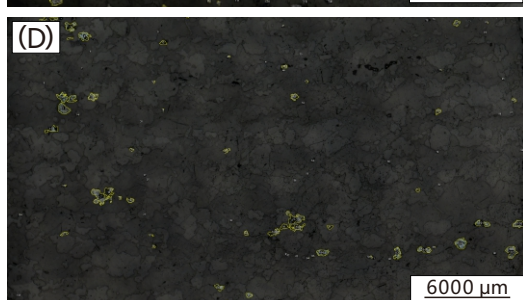
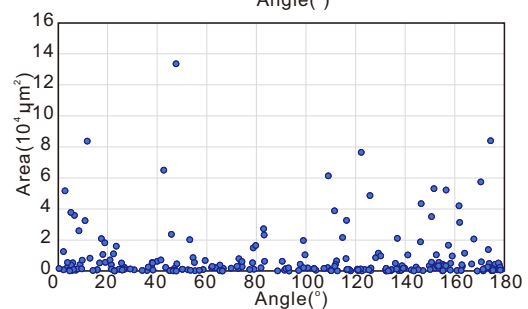
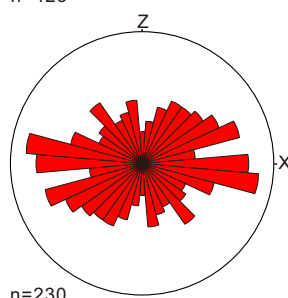
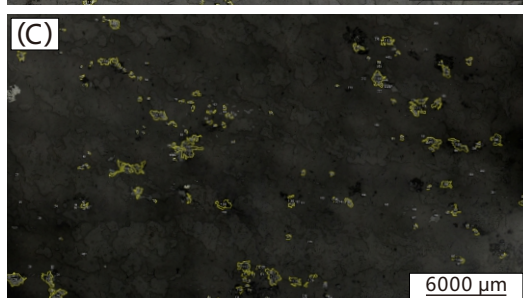
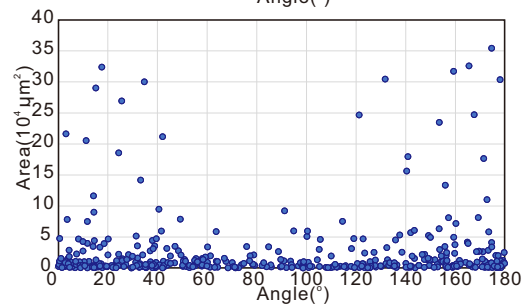
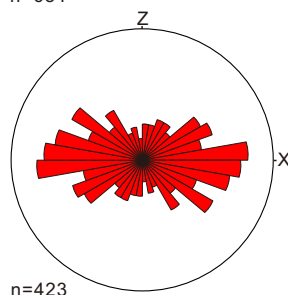
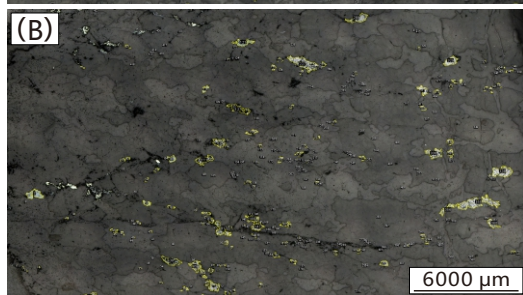
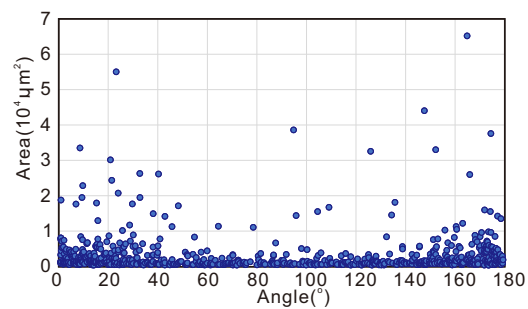
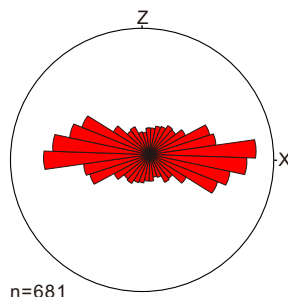
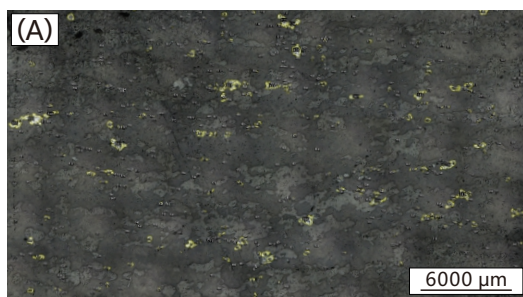
Table S1. Anisotropy of magnetic susceptibility (AMS) measurements for the Hadabei dome.

Supplemental Data S1. Data for shape fabric analysis.

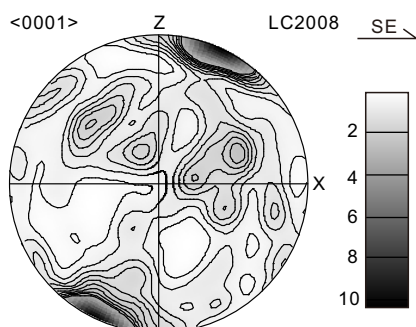
Supplemental Data S2. Geochronology data for samples XY18015-C and XY17008-3.



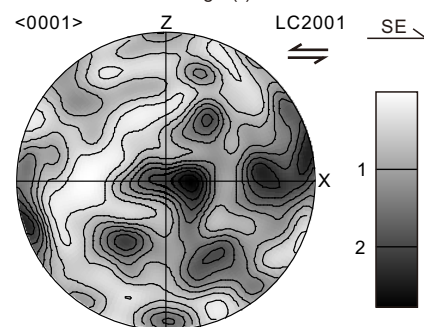




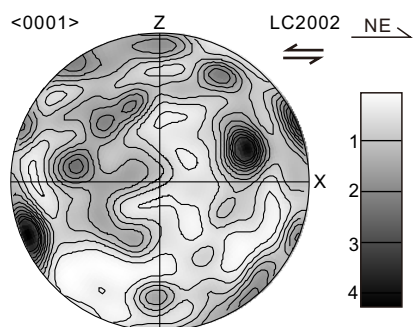
Quartz 202 data points Exp. densities (mud):
Min= 0.01, Max= 3.19



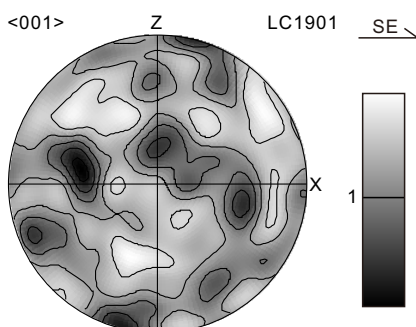
Quartz 212 data points Exp. densities (mud):
Min= 0.02, Max= 10.35



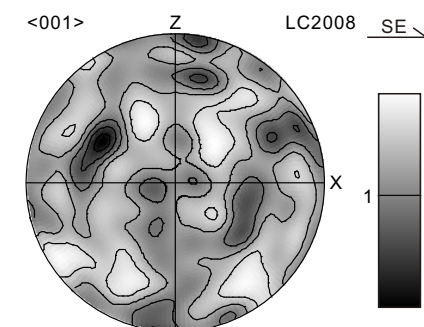
Quartz 179 data points Exp. densities (mud):
Min= 0.04, Max= 2.79



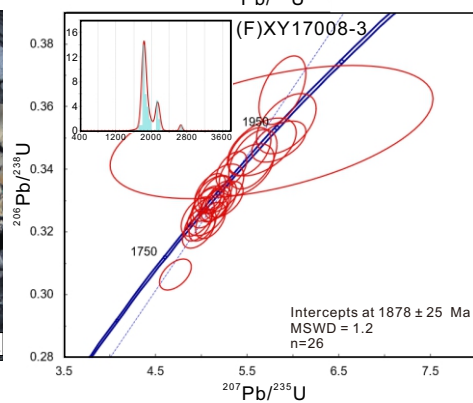
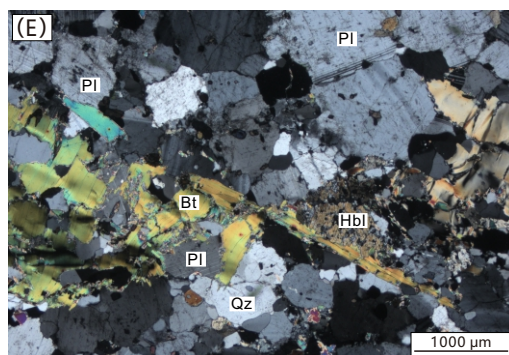
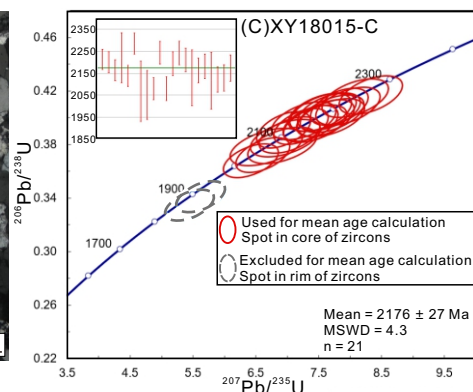
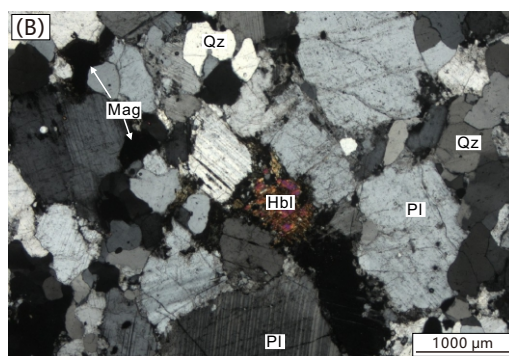
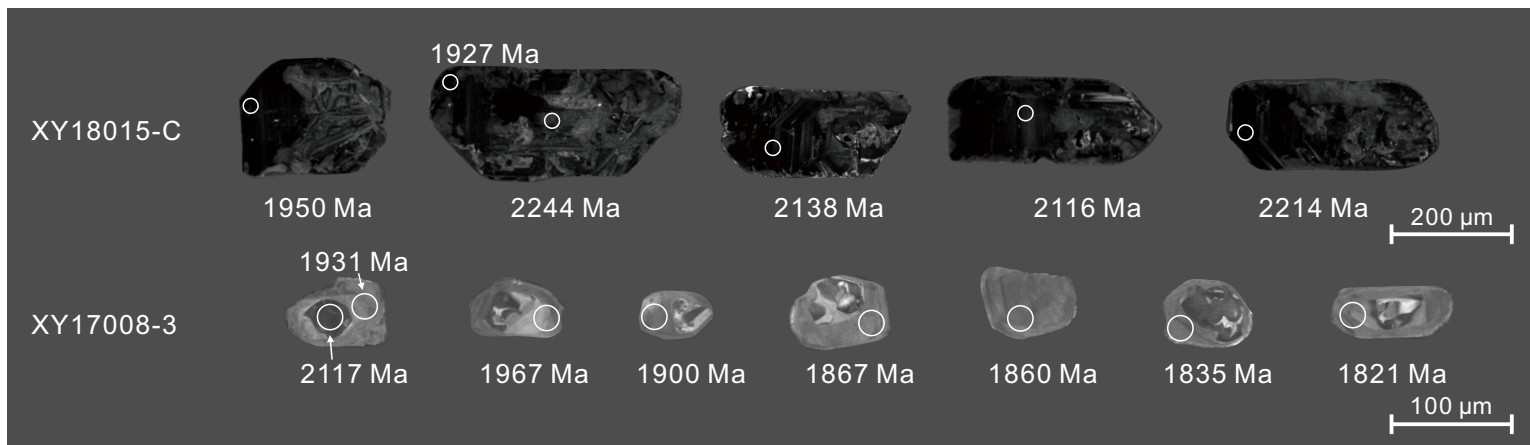
Quartz 211 data points Exp. densities (mud):
Min= 0.05, Max= 4.25



Magnetite 173 data points Exp. densities (mud):
Min= 0.37, Max= 2.04



Magnetite 160 data points Exp. densities (mud):
Min= 0.37, Max= 2.10



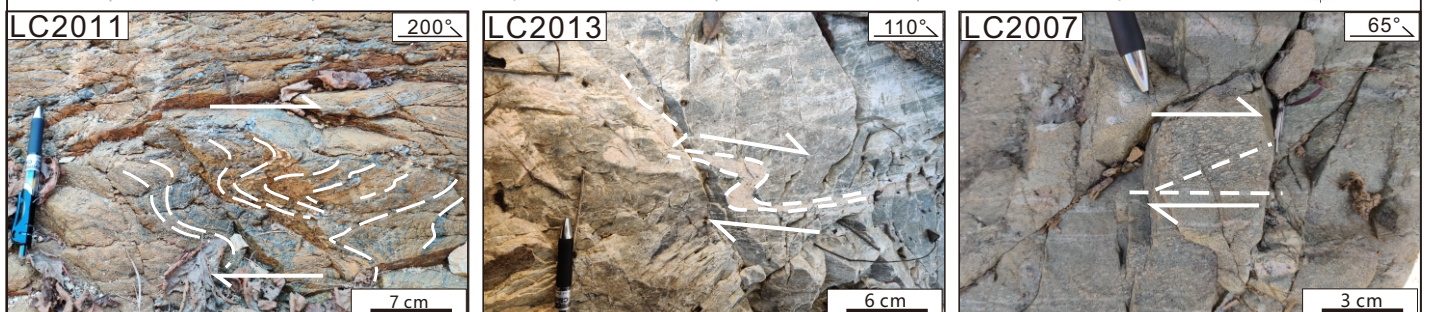
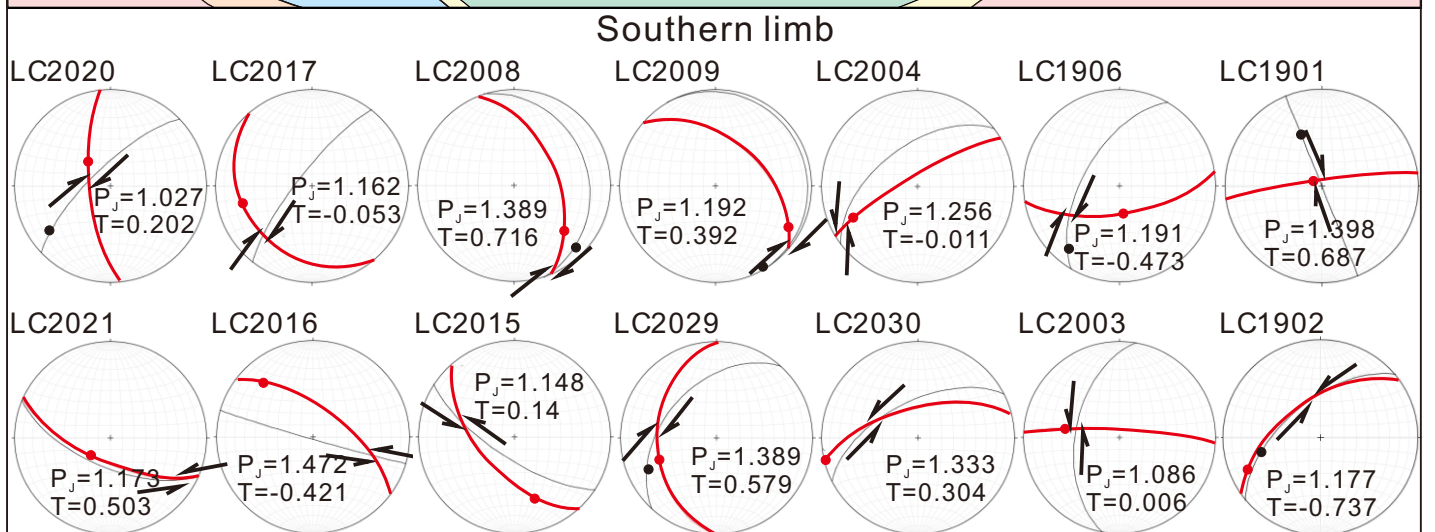
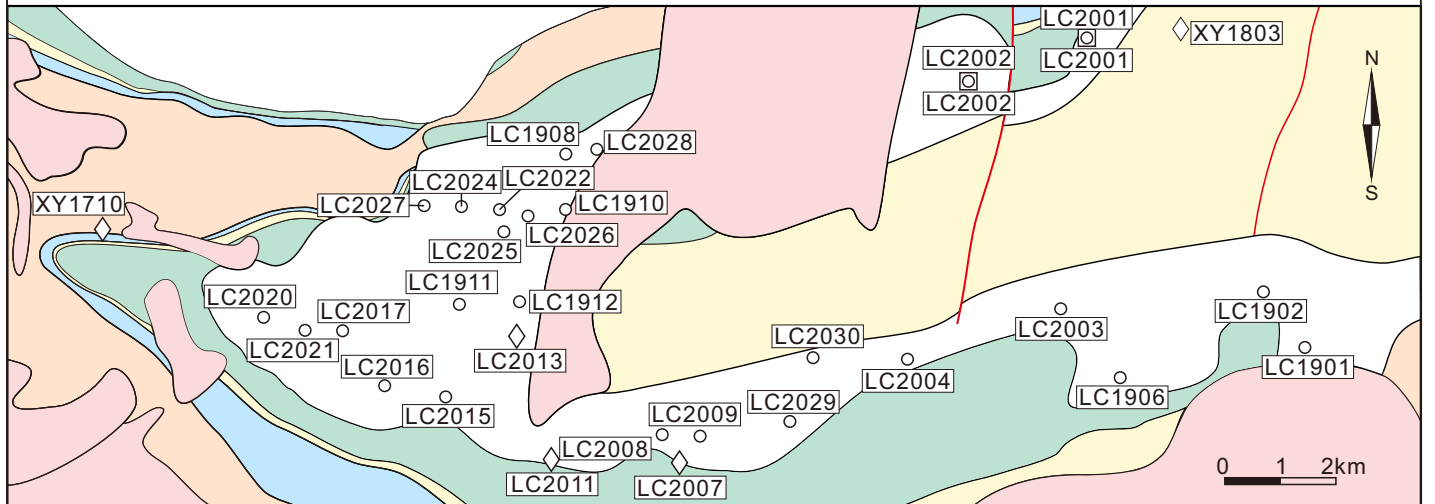
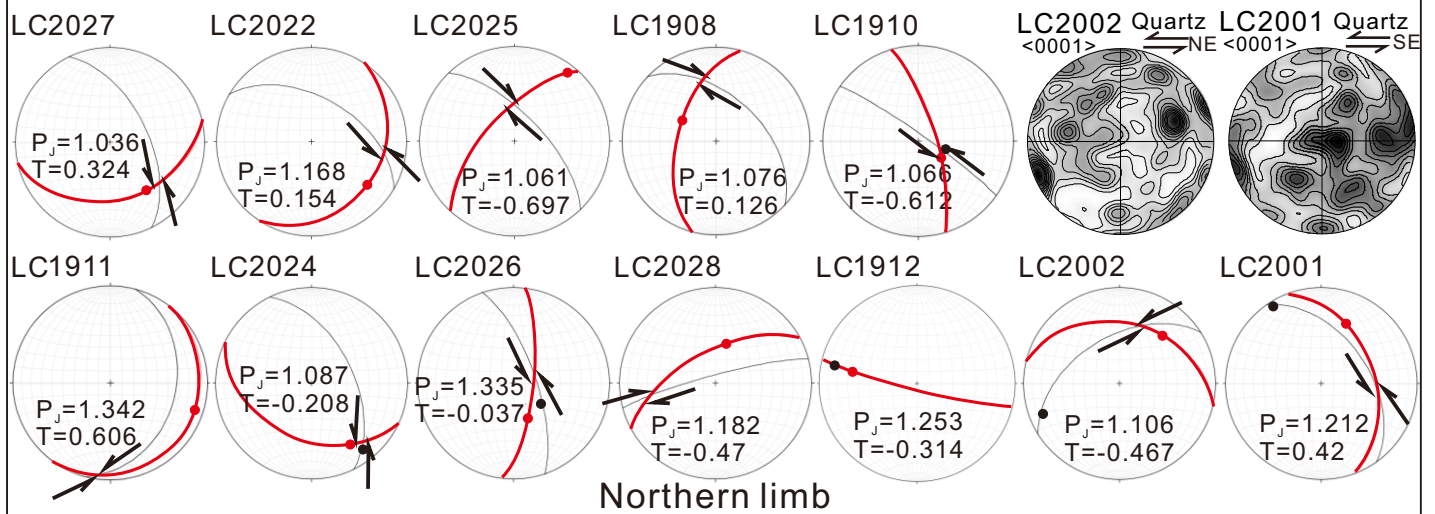
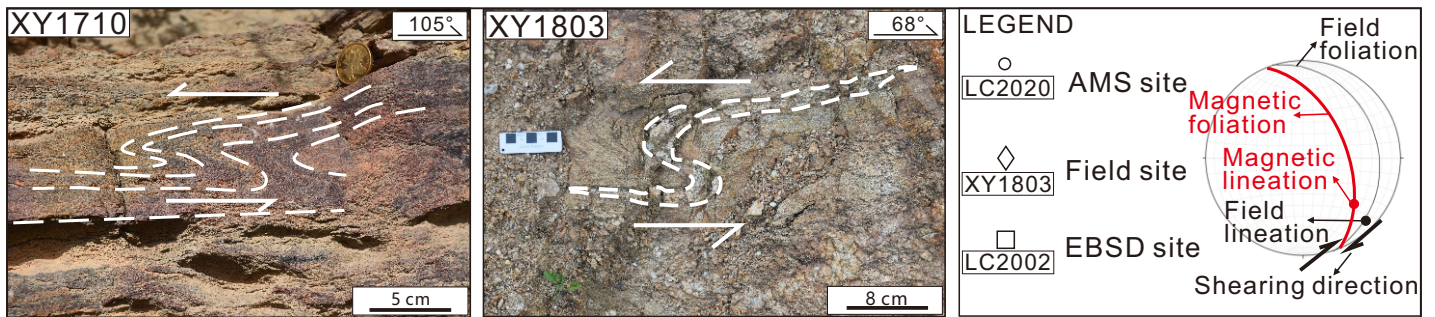


Figure S1. Dependence of the magnetic susceptibility with temperature for representative samples of the Liaoji granitic gneisses (dark line shows the heating process, whereas light line shows the cooling process). (A) Sample LC1901. (B) Sample LC2001. (C) Sample LC2002. (D) Sample LC2008. (E) Sample LC2026. (F) Sample LC2029. The irreversible thermomagnetic curves of the samples (except for sample LC2001) during cooling indicate the formation of new magnetic minerals by heating. Considering that there are a few hematite grains in the samples, the above characteristics may be attributed to the transformation of hematite into maghemite or magnetite.

Figure S2. Magnetic fabric (A) and field fabric (B) of the Hadabei dome. C-E. Anisotropy of magnetic susceptibility results for the Liaoji granitic gneisses samples of the Hadabei dome. (C) The relationship between the bulk magnetic susceptibility and the degree of magnetic anisotropy. (D) The relationship between the bulk magnetic susceptibility and the shape parameter. (E) The relationship between the degree of magnetic anisotropy and the shape parameter.

Figure S3. Shape preferred orientation of magnetite grains and area vs. angle diagrams, and the crystallographic preferred orientation of quartz and magnetite in the Liaoji granitic gneisses. (A) Sample LC1901. (B) Sample LC2008. (C) Sample LC2026. (D) Sample LC2029. Pole figures are plotted in lower hemisphere equal-area projections, X-lineation direction, Z-normal to the foliation plane.

Figure S4. Field appearance, microscopic characteristics, CL image and zircon U-Pb Concordia diagrams of the dating samples from the Hadabei dome. (A) XY18015-C, Liaoji granitic gneisses. (B) The photomicrograph of XY18015-C. (C) Zircon U-Pb Concordia diagrams of XY18015-C. (D) XY17008-3, migmatites. (E) The photomicrograph of XY17008-3. (F) Zircon U-Pb Concordia diagrams of XY17008-3. Qz-quartz; Pl-plagioclase; Bt-biotite; Hbl-hornblende; Mag-magnetite. MSWD-mean square of weighted deviates.

Figure S5. Kinematic map of the northern and southern limbs of the Hadabei dome, with the locations of AMS, field and EBSD sites.

SUPPLEMENTAL TEXT: FABRIC ANALYSIS AND GEOCHRONOLOGICAL DATING: SAMPLES AND METHODS

Samples

In this study, AMS is selected as the method to collect the magnetic data of the Liaoji granitic gneisses, which is used to analyze the kinematic characteristics of shearing of the Liaoji granites by combining the AMS results, field and microstructural observations. The AMS measurements for the Hadabei dome are given in Supplemental Table S1 in the Supplemental Material. Two U-Pb ages of zircon were determined in this study. The sample XY18015-C was collected from the granitic core of the Hadabei dome, and the sample XY17008-3 was taken from migmatites near the core.

Magnetic Mineralogical Analysis

We performed magnetic mineralogy investigations using thermomagnetic curves in order to better understand the AMS results. The thermomagnetic curves were measured at low- to high-temperature using powdered samples in the CS-3 apparatus coupled to the KLY-4S Kappabridge (AGICO, Czech Republic). All thermomagnetic curves were performed at a temperature interval from 0 °C to 700 °C. All measurements were carried out in the Paleomagnetism and Environmental Magnetism Laboratory, China University of Geosciences, Beijing.

Anisotropy of Magnetic Susceptibility

A total of 146 specimens were collected from 26 stations throughout the granitic core of the Hadabei dome for magnetic analysis. Each specimen was cut into standard specimens that were 2 cm in length and 2.54 cm in diameter. All measurements were carried out in the Paleomagnetism and Environmental Magnetism Laboratory, China University of Geosciences, Beijing. Measurements of magnetic susceptibility were carried out on a KLY-4S Kappabridge (AGICO, Czech Republic) with a working frequency of 875 Hz and a field intensity of 300 A/m. The results of magnetic measurements for station averages are summarized in Table S1, and the magnetic fabrics are given in Figure S5.

Shape Fabric Analysis

Four samples from the Hadabei dome were used for analysis of shape fabrics of magnetite grains in the granites. Thin sections were cut perpendicular to the foliation and parallel to the lineation (XZ plane). Images were taken using Reflected Light Microscope. The length and orientation of the long and short axes, areas and other data of the grains were collected through shape fabric analysis. The orientation rose diagrams were drawn from these data. Data for shape fabric analysis are listed in Supplemental Data S1.

Lattice-preferred Orientation (LPO) Fabric Analysis

Lattice-preferred orientation (LPO) fabric analyses of quartz and magnetite from 4 samples were completed at the Rock Fabrics Laboratory, China University of

Geosciences, Beijing. The sections were polished using Buehler Mastermet colloidal silica and a Buehler grinder/polisher. The LPO data acquisition was performed on a Hitachi S-3400N II scanning electron microscope equipped with a Nordlys EBSD Model NL-II detector with the section surface inclined at 70° to the incidental beam. An accelerating voltage of 15 kV and a working distance of 19.2 mm was used. EBSD analysis was performed using the HKL Channel 5 software package.

Zircon U-Pb Age Dating

Cathodoluminescence (CL) techniques were taken to examine the internal structure of the zircon grains. The U-Pb analyses were carried out on the LA-ICP-MS at the Elemental Geochemistry Laboratory, China University of Geosciences, Beijing. The laser model is LSPC-193-SS made by EAST LASER Corporation. The velocitron model is Elite made by Jena Corporation in Germany. The standard zircons 91,500 were employed as external standard and 91500 (B), TEMORA, or Qinghu were employed to monitor isotopic ratios (age). Data were processed by Glitter 4.4.4 software on the special computer of the Elemental Geochemistry Laboratory, China University of Geosciences, Beijing. Laser ablation-inductively coupled plasma-mass spectrometry (LA-ICP-MS) U-Pb zircon data of the samples are listed in Supplemental Data S2.

TABLE S1. ANISOTROPY OF MAGNETIC SUSCEPTIBILITY (AMS) MEASUREMENTS FOR THE HADABEI DOME

Locality	N	Mineral	Km (μ SI)	F	L	P _J	T	K _{1dec}	K _{1inc}	K _{2dec}	K _{2inc}	K _{3dec}	K _{3inc}
LC1901	5	Mag+Hbl	51900	1.300	1.050	1.398	0.687	304.4	81.7	78.1	5.7	168.7	5.9
LC1902	10	Mag+Hbl+Bt	15600	1.020	1.139	1.177	-0.737	247.1	20.2	4.7	51.4	144.2	31.2
LC1906	8	Mag+Hbl	64000	1.045	1.132	1.191	-0.473	162.8	65.6	259.8	3.2	351.2	24.1
LC1908	5	Mag+Hbl	22200	1.042	1.032	1.076	0.126	302.5	55.0	200.4	8.4	104.8	33.7
LC1910	5	Mag+Hbl	22800	1.012	1.050	1.066	-0.612	120.6	66.9	348.0	16.1	253.2	16.1
LC1911	5	Mag+Bt	22300	1.250	1.056	1.342	0.606	107.2	9.8	197.9	3.7	308.2	79.5
LC1912	5	Mag	42700	1.079	1.157	1.253	-0.314	279.8	36.0	97.7	54.0	189.1	1.0
LC2001	5	Mag+Hbl	41400	1.142	1.056	1.212	0.42	22.6	33.7	130.8	25.1	249.5	45.7
LC2002	6	Mag+Hbl	2400	1.026	1.074	1.106	-0.467	42	33.1	302.7	13.9	193.3	53.4
LC2003	5	Mag	18900	1.042	1.042	1.086	0.006	280	43.2	85.8	45.9	183.2	7.1
LC2004	5	Mag	17300	1.119	1.122	1.256	-0.011	244	26.9	42.1	61.4	149.3	9.2

LC2008	6	Mag	63300	1.298	1.044	1.389	0.716	131.5	30.6	14.2	37.8	248.2	37.2
LC2009	6	Mag	31700	1.127	1.053	1.192	0.392	118.9	14.7	12.8	46.7	221.4	39.6
LC2015	6	Mag+Bt	21800	1.082	1.061	1.148	0.14	161	33.2	287.4	42.2	48.8	29.9
LC2016	6	Mag	54400	1.115	1.306	1.472	-0.421	318	23.2	84.9	54.5	216.3	25.2
LC2017	5	Mag+Hbl	17500	1.074	1.082	1.162	-0.053	256.6	26.2	160.9	11.4	49.4	61.1
LC2020	6	Hbl+Bt	160	1.016	1.011	1.027	0.202	318.2	61.3	181.7	21.7	84.4	17.9
LC2021	5	Mag	46600	1.122	1.039	1.173	0.503	226.8	67.6	117.2	7.9	24.2	20.9
LC2022	5	Mag+Bt	28300	1.093	1.068	1.168	0.154	127.8	26.7	36.9	1.8	303.4	63.2
LC2024	5	Bt	1260	1.033	1.051	1.087	-0.208	147.9	25.1	253.4	29.8	25.1	49.2
LC2025	5	Bt	68.6	1.008	1.047	1.061	-0.697	38.6	8.8	290.4	63.7	132.7	24.5
LC2026	7	Mag+Bt	59900	1.149	1.162	1.335	-0.037	157.4	57.4	15.5	26.7	276.5	17.3
LC2027	5	Bt	1690	1.023	1.012	1.036	0.324	142.1	36.5	241.1	12	346.2	50.9
LC2028	5	Mag+Bt	74700	1.044	1.126	1.182	-0.47	14.6	55.1	251.8	20.7	150.8	26.7

LC2029	5	Mag	19900	1.279	1.068	1.389	0.579	248.3	35.9	346.6	11.3	91.3	51.8
LC2030	5	Mag+Hbl	40500	1.203	1.103	1.333	0.304	256.6	1.8	350.5	65.2	165.7	24.7

Note: N-number of specimens measured; Mineral-the main composition of dark minerals, Mag-magnetite, Hbl-hornblende, Bt-biotite; F-degree of magnetic foliation; L-degree of magnetic lineation; P_j-corrected anisotropy degree; T-shape parameter; K₁-trend and plunge of magnetic lineation; K₂-trend and plunge of the intermediate axis; K₃-trend and plunge of the pole of the magnetic foliation.
